渣金间辅助外电场提高焊接工艺稳定性分析

李晓泉， 杨宗辉， 赵治国
(南京工程学院 材料工程学院，南京 211167)

摘 要：为探索焊接过程实现高稳定性工艺的潜在途径，最大限度地减少重要钢结构制造中焊缝咬边及成形缺陷带来的焊后返修工作，提出并试验了一种利用埋弧焊渣金间随焊施加辅助外电场对渣金电导载流进行导流，进而提高焊接工艺稳定性的方法，并应用焊接电信号分析仪对弧压信号进行了采集统计分析. 结果表明，以钨电极作阴极利用电场在渣金熔体内部形成稳定的电导载流，可使熔渣电导性能得以改善，并引导电子进入电弧阴极中心以增强电弧的集聚程度. 同时外电场作用也使渣金内部的带电粒子形成有序运动并在界面结合成低表面能的活性氧化物，又可改善液态熔渣在焊缝金属表面的润湿铺展性能. 实施辅助电场引入的这些有益作用使焊缝形状、表面光洁度、尤其是焊缝边缘平直均匀性得到较好地改观，焊接过程工艺稳定性得以进一步提高.

关键词：外电场；埋弧焊；焊接工艺；稳定性
中图分类号：TG409 **文献标识码**：A **文章编号**：0253－360X(2014)01－0017－04

0 序 言

目前大型化工压力容器的建造大量应用高效大能量埋弧自动焊接. 压力容器制造一般都要求采用工艺性能较差的碱性烧结焊剂进行焊接，但对焊缝表面质量诸如焊道咬边深度、焊缝余高、焊缝宽度的均匀性以及焊缝表面光洁度等又有较高的要求. 为此通过进一步提高焊接过程工艺稳定性，最大限度地控制焊缝形成过程的波动，可以有效地减少焊后返修工作量从而提高生产效率.

根据熔渣的离子特性，熔渣在熔融状态本身具有一定的导电性能. 目前，充分利用熔渣的这种性能实现无污染脱氧在炼钢冶金领域已成为新的研究热点[1－3]. 由于焊接冶金过程与炼钢冶金过程在本质上具有相似之处，若能对焊接过程中熔渣及液态金属内部电导载流体的有序运动加以有效地利用，将有可能从一个全新的角度开辟焊接冶金质量控制的新途径. 作者已对焊接熔渣在通电条件下与液态金属间的电化学作用进行了一些探索，并就埋弧焊夹杂物的形成机制及渣金间外加电场控制焊缝金属氧化物夹杂开展了一些试验研究[4－6]. 初步研究发现，在一定条件下外电场对焊接工艺还存在一些有益作用，具有一定的潜在应用价值. 文中报道了试验涉及的埋弧焊渣金间外加电场对焊接工艺稳定性的影响，并从机理上作了深入探讨.

收稿日期：2013－03－20
基金项目：国家自然科学基金资助项目(51075197)；江苏省科技支撑工业计划资助项目(BE2012186)

1 试验方法

试验设备用 MZ-1250 型埋弧焊机，电源极性采用直流反接法，以行走小车进行自动焊接. 焊接材料为 SJ101 烧结焊剂配合直径 4 mm 的 H10Mn2 焊丝. 焊接时在厚度为 14 mm 的 Q235 钢板上进行表面堆焊，焊接工艺参数为焊接电流 600～610 A，电弧电压 30～34 V，焊接速度 33 cm/min.

辅助外电场的施加方法如图 1 所示，以 30 V/50 A 的直流电源提供外电场. 直流电源的输出端一极接直径 3.2 mm 的铈钨电极，而另一输出极与被焊母材接通. 变换 K_1 可改变辅助电源的输出极性. 将铈钨电极用有机绝缘夹具固定在行走机头中且与焊丝导电嘴相互绝缘，并可进行上下高度调节. 试验前通过试焊观察直流电源的电流信号调整钨电极上下高度，使其正好插入电弧外围的液态熔渣内部，但又未进入熔池造成短路. 焊接时接通辅助电源，铈钨电极随同机头向前移动，这样即在熔渣与熔池之间施加了一辅助外电场. 在其它工艺条件完全相同进行施加和不施加外电场焊接试验. 焊后对焊缝金属用光谱仪作成分分析，焊渣经研磨成细粉后作 X 射线衍射相结构分析. 为探讨外电场作用对焊接电弧的影响，应用自行组装焊接电信号分析仪对焊接过程电弧电压进行数据采集. 该分析仪的系统硬件结构如图 2 所示，采用 LabVIEW 8.2 作为开发平台，对

焊接电弧电压以 10 kHz 频率进行数据采集，然后将采集得到的数据进行综合分析处理. 由于埋弧焊过程熔滴过渡具有周期性特征，焊接电弧电压信号呈现锯齿状的波形，根据该波形很难区分比较两者的不同之处. 试验采用对采集的电弧电压信号作概率密度分布统计分析，以比较施加外电场和不施加外电场信号的变化情况.

(a) 钨电极安放实物图

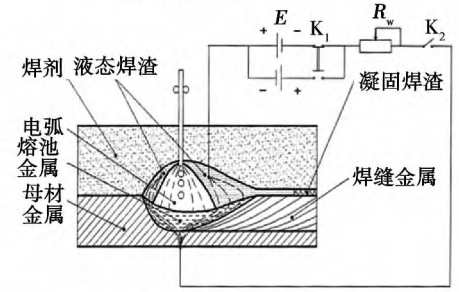

(b) 辅助外电场施加原理图

图 1 渣金间辅助外电场施加原理图

Fig. 1 Schematic of applying auxiliary electric field between slag and metal

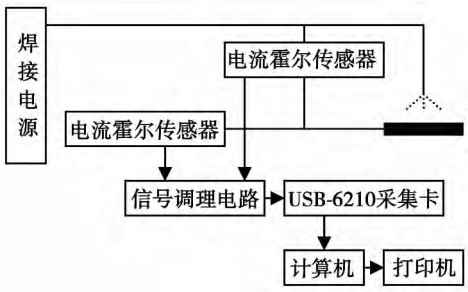

图 2 系统硬件结构示意图

Fig. 2 Structure of system hardware

2 试验结果及分析讨论

2.1 外加电场施加效果试验

试验显示，辅助电源的输出极性在一定程度上影响到外电场的施加效果. 当外加辅助电源的正极与钨电极相接时，渣金间作用的电压不稳定，相应的电流波动较大. 但当改变辅助电源的极性，使其负极与钨电极连通，此时设置辅助电源开路电压为 20 ~ 30 V，渣金间即可形成十分稳定的 5 ~ 8 A 的辅助电流，与此同时，渣金间的电压也下降并稳定在 10 ~ 12 V. 当外加辅助电源的开路电压设置为零时，测试出渣金间的电流仍为零，表明未施加外电场时渣金间并未形成稳定的离子流向.

钨电极的插入位置也对辅助电流的形成构成较大的影响. 由于焊剂仅在熔融状态才具有导电性能，当辅助电源的电流显示为零，而电压显示为开路电压时，表明此时钨电极尚未插入熔渣内部. 当辅助电源电流显示为 22 ~ 25 A，电压显示接近于零时，则表明电极已插入熔池金属造成了短路. 因此，根据渣金间流经的电流及相应的电压信号，可以对钨电极的插入位置进行有效地控制.

通常情况下，熔渣由金属阳离子、硅氧复合阴离子及自由氧离子组成. 熔渣的导电性能主要取决于熔融的氧化物在高温条件下电离出的离子电导，而液态金属由于保存有固态金属键，其导电性能则取决于内部的电子电导[7]. 相比之下，熔渣的导电性能远不如熔池金属. 当渣金间施加一外电场且铈钨电极作阴极时，试验显示，一旦将铈钨电极与导电嘴短路即可诱发两者间产生电弧. 同时改变辅助电场的极性焊接又导致渣金间电流不稳定，表明铈钨电极表层不存在负电层因而无电场电子发射时，熔渣内部仅靠离子电导，难以维持电流的稳定. 据此即可判断外加电场作用可以使具有较低电子逸出功的铈钨电极尖端电场发射一定的电子，以增加熔渣的电导性能.

2.2 外电场对焊缝成形的影响

图 3 为在外电源开路电压设置为 30 V、钨电极接负极条件下，渣金间流经 7 ~ 8 A 的稳定电流时，施加外电场和未施加外电场作用得到的焊缝成形对比. 表 1 为相应焊缝及母材化学成分的分析结果. 试验结果显示，施加外电场作用后，焊缝边缘明显变得更为平直，焊址部位焊缝与母材的齿合镶嵌现象得到较好的改善，焊道宽窄均匀性显著提高，宽度略为变窄; 同时焊缝表面光洁度也得到改观，焊缝中心轴线两侧对称性十分良好，横截面呈现更为明显的圆弧形状. 上述焊缝成形可防止咬边缺陷，是一种高稳定性焊接工艺的焊缝成形.

焊缝成形的改善主要得益于施加外电场对焊接主电路起到有导流稳弧效应. 对于直流反极性的埋弧焊接而言，作为焊接电弧阴极的熔池金属与施加的外电场阳极实际上是共用极. 这样就形成一个由

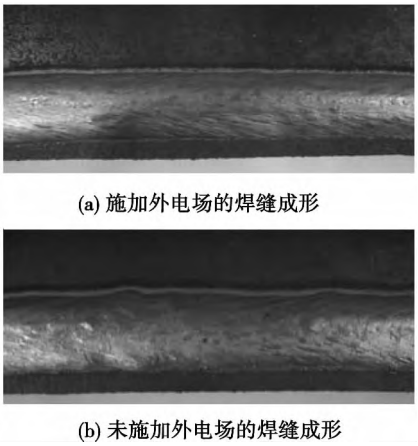

(a) 施加外电场的焊缝成形

(b) 未施加外电场的焊缝成形

图 3　辅助电场作用对焊缝成形的影响

Fig. 3　Influence of auxiliary electric field on weld appearance

表 1　焊缝及母材金属化学成分分析结果(质量分数，%)

Table 1　Results of chemical compositions analysis for weld and base metal

分析项目	C	Mn	Si	S	P
未施外场焊缝	0.109	0.951	0.319	0.021	0.033
施加外场焊缝(电压 25 V)	0.107	0.982	0.293	0.021	0.034
施加外场焊缝(电压 30 V)	0.103	0.909	0.279	0.020	0.032
母材金属	0.172	0.370	0.185	0.019	0.021

外电场阴极→电弧阴极→电弧阳极的电势差. 铈钨电极与焊接机头导电嘴短路可引发电弧即可证实上述电势差的存在. 由此铈钨电极发射出的电子势必将逆着这一电势差由熔渣流向焊接电弧的阴极. 同时外加电场作用导通渣金电子通道后在铈钨电极和电弧阴极间增加了一个 10 ~ 12 V 的额外电压，该外电压相对于 30 ~ 32 V 的电弧电压已是一个不容忽视的额外压差，这相当于增设了一个使熔池内部电子流向电弧阴极的动力“泵”，使电弧阴极发射电子更加集中于电弧阴极中心. 另外铈钨电极安放于熔化焊丝后部紧邻电弧的熔渣内部且始终处于焊缝轴线中心，这更加有利于熔池中电子向电弧中心集聚从而增加电弧的集聚程度，电弧中心集聚度的提高易于形成几何形状更为稳定的熔池. 这在一定程度上克服了电弧边缘波动引起熔化金属不均匀现象，因而形成的焊缝边缘平直度显著增加，大大消除了焊道与母材的齿合镶嵌现象，有利于防止咬边缺陷的发生.

根据表 1 的化学成分分析结果，施加外电场的焊缝金属与未施加外电场的焊缝金属相比，硅含量有所下降，而锰含量几乎没有变化. X 射线衍射分析也证实前者形成的焊渣中 SiO_2 比例较后者有所提高. 对于氟碱型的 SJ101 烧结焊剂，其造渣剂主要由 MgO，CaO，Al_2O_3 碱性氧化物、CaF_2 去氢组分及少量的 SiO_2 酸性氧化物组成，冶金过程采用 Si-Fe，Mn-Fe 进行脱氧及过渡合金. 渣金间外电场作用促使熔渣中自由氧离子向渣金界面迁移，在此过程中，与氧亲和力最强的硅将优先在界面与氧结合形成具有共价键的 SiO_2 低表面能活性物质. 考虑到碱性烧结焊剂主要由表面张力较大的 MgO，CaO 离子键物质组成，相对于酸性熔渣而言对焊缝金属的润湿铺展能力较弱，而熔池凝固过程中利用外电场的诱导作用直接在渣金界面形成低表面能的活性 SiO_2 薄膜将有利于改善液态熔渣在焊缝表面的润湿铺展性能，因此在一定程度上也使焊缝表面光洁度及焊缝边缘平直度得到提高. 同时施加外电场可抑制焊缝金属增硅，这也为控制焊缝金属因增硅而导致脆化提供了一条冶金电化学新思路.

2.3　弧压信号统计分析

图 4 为用弧焊分析仪对施加外电场和不施加外电场两种条件下焊接电弧电压实时采集，进而统计出的各种电压值的概率密度分布曲线. 从弧压信号统计出的电弧电压概率分布密度来看，施加外电场后概率密度分布曲线有向左“漂移”的趋势，特别是作为概率取值最大的峰值存在一定的向低压方向移动的现象. 表明电弧向中心区域集聚后维持电弧稳定燃烧所需的电压自发有所降低. 同时施加外电场作用后，高电弧电压区域的概率也更低，这也说明施加外电场作用后电弧电压更易于在低值状态下维持电弧的稳定燃烧. 一般来讲，电弧电压呈现低值伴随着电弧空间集聚有较多的导电载流子，故只需较低的电压就足以维持电弧的稳定燃烧. 反之当电弧空间的导电载流子不足时，则必需提高电弧电压以增强电离及电子发射作用，才能维持电弧的稳定燃烧. 从弧压信号的统计分析结果也可进一步证实外电场的导流作用使熔池发射电子更多集聚于电弧中心区域从而产生一定的稳弧效应.

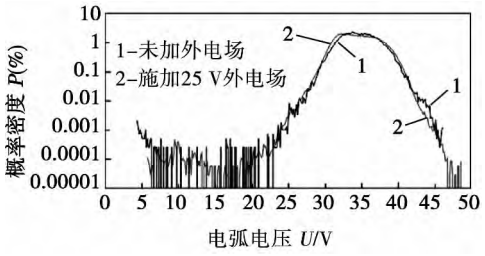

图 4　焊接电弧电压概率密度分布

Fig. 4　Probability density distribution of welding arc voltage

3 结 论

(1) 从冶金电化学角度提出并试验了一种利用铈钨电极材料作阴极,在埋弧焊渣金间随焊施加辅助外电场以提高焊接工艺稳定性的方法.

(2) 利用铈钨作阴极的辅助外电场对直流反接埋弧焊工艺稳定性能的改善主要基于电场作用可形成稳定的电导载流,同时有效地改善液态熔渣的导电性能,并可引导熔池中电子流向电弧阴极中心进而增强焊接电弧的集聚度.

(3) 外电场诱发的电化学作用促使 Ti,Al,Si 等亲氧元素在渣金界面形成低表面能的活性氧化物,有利于熔渣润湿铺展均匀,以获得更为光洁圆滑的焊缝形状.

参考文献:

[1] 鲁雄刚,梁小伟,袁 威,等. 渣金间外电场无污染脱氧法的研究[J]. 金属学报,2005,41(2):113-117.
Lu Xionggang, Liang Xiaowei, Yuan Wei, *et al*. Study of unpolluted deoxidization method with applied voltage between metal and slag [J]. Acta Metallurgica Sinica, 2005, 41(2): 113-117.

[2] 李建朝,张捷宇,鲁雄刚,等. 渣金间外加直流电场无污染脱氧[J]. 过程工程学报,2006,6(增刊1):30-34.
Li Jianchao, Zhang Jieyu, Lu Xionggang, *et al*. Unpolluted deoxidization of molten steel with applied DC voltage between metal and slag [J]. The Chinese Journal of Process Engineering, 2006, 6(Suppl. 1): 30-34.

[3] 高运明,姜 英,张 华,等. 可控氧流冶金[J]. 武汉科技大学学报(自然科学版),2007,30(5):449-453.
Gao Yunming, Jiang Ying, Zhang Hua, *et al*. Metallurgy with controlled oxygen flow [J]. Journal of Wuhan University of Science & Technology (Natural Science Edition), 2007, 30(5): 449-453.

[4] 李晓泉,初雅杰,杨宗辉. 电化学作用对直流焊接熔滴金属致氧量的影响[J]. 焊接学报,2010,31(1):29-32.
Li Xiaoquan, Chu Yajie, Yang Zonghui. Influence of electrochemical reaction on oxygen pick-up for droplet metal in direct current welding [J]. Transactions of the China Welding Institution, 2010, 31(1): 29-32.

[5] 李晓泉,初雅杰,杨宗辉,等. 电弧焊熔滴金属中夹杂物形成的冶金机制[J]. 焊接学报,2010,31(10):5-8.
Li Xiaoquan, Chu Yajie, Yang Zonghui, *et al*. Metallurgical mechanism of inclusion forming in droplet metal with arc welding [J]. Transactions of the China Welding Institution, 2010, 31(10): 5-8.

[6] 李晓泉,初雅杰,杨宗辉. 焊缝金属氧化物夹杂尺寸及分布的辅助外电场控制法[J]. 焊接学报,2013,34(10):5-8.
Li Xiaoquan, Chu Yajie, Yang Zonghui. Size and distribution controlling method of oxide inclusions in weld metal with auxiliary electric field [J]. Transactions of the China Welding Institution, 2013, 34(10): 5-8.

[7] 鲁雄刚,蒋国昌,李福燊,等. 熔渣体系电子电导的研究[J]. 中国稀土学报,1998,16(专辑):457-462.
Lu Xionggang, Jiang Guochang, Li Fushen, *et al*. A study on the electronic conductivity of the slag system [J]. Journal of the Chinese Rare Earth Socity, 1998, 16(Spec. Issue): 457-462.

作者简介: 李晓泉,男,1964 年出生,博士,教授,硕士研究生导师. 主要从事焊接冶金及新型材料连接领域的科研和教学工作. 发表论文 50 余篇. Email: lixq@njit.edu.cn

MAIN TOPICS, ABSTRACTS & KEY WORDS

Characteristic of fusion-brazed joint between 5052 aluminum alloy and zinc-coated steel by CO_2 laser FAN Ding[1,2], JIANG Kai[1], YU Shurong[1,2], ZHANG Jian[1] (1. State Key Laboratory of Gansu Advanced Non-ferrous Metal Materials, Lanzhou University of Technology, Lanzhou 730050, China; 2. Key Laboratory of Non-ferrous Metal Alloys and Processing of Ministry of Education, Lanzhou University of Technology, Lanzhou 730050, China). pp 1 - 4

Abstract: Welding between aluminum and steel has become a hot and difficult problem in the field of welding. By means of CO_2 laser welding and brushing metal powder and flux before welding, overlap fusion-brazed joint between 5052 aluminum alloy and ST04Z zinc-coated steel sheets was obtained, in which the 5052 aluminum alloy was melted but zinc-coated sheet was brazed. The microstructure in the joint and fracture features of the tensile specimen were investigated by optical microscope, scanning electron microscope (SEM) and universal testing machine. The results indicate that after brushing metal powder and flux, the laser absorption could be improved greatly, and the resultant weld appearance was sound and the zinc-coated layer was not burned. The thickness of the intermediate layer was less than 10 μm, and acicular intermetallic compounds did not diffuse into the aluminum weld. The maximum tensile strength of the joint was 208 MPa, about 95% of 5052 aluminum alloy.

Key words: aluminum alloy and steel; laser welding; fusion-brazing; metal powder

Characteristics of welding arc during ultrasound-MIG hybrid welding of aluminum alloy FAN Chenglei[1], XIE Weifeng[1], YANG Chunli[1], KOU Yi[2] (1. State Key Laboratory of Advanced Welding and Joining, Harbin Institute of Technology, Harbin 150001, China; 2. Changchun Faw-Volkswagen Automotive Co., Ltd, Changchun 130011, China). pp 5 - 8

Abstract: In order to better understand the ultrasound-MIG welding process, the arc behavior during ultrasonic-MIG welding of aluminum alloy was investigated in this paper. The response of ultrasound-arc was explored at different wire feeding speeds or welding voltages. The results show that the compression effects of ultrasound-arc varied with different welding parameters. With the increase of wire feeding speed, the compression gradually became weaker. According to the results, the analysis of ultrasound-arc self-adjusting was carried out. Compared with the traditional MIG welding, the electric field strength and temperature in ultrasonic arc were greatly enhanced and led to stronger welding stability.

Key words: arc compression; electric field intensity; particle motion; temperature field; self-regulation

Microstructure and shear strength of high-temperature brazed joint of Super-Ni/NiCr laminated composite using Ni-Cr-Si-B filler metal WU Na, LI Yajiang, WANG Juan (Key Laboratory for Liquid-Solid Structural Evolution and Processing of Materials (Ministry of Education), Shandong University, Jinan 250061, China). pp 9 - 12, 36

Abstract: Super-Ni/NiCr laminated composite and Cr18-Ni8 steel were brazed with Ni-Cr-Si-B high-temperature brazing filler metal. The microstructure, phase constitution, shear strength and fracture morphology were analyzed. The brazed region consisted of γ-Ni solid solution, Ni_3B, CrB and Ni_3Si. The microhardness fluctuated across the brazed region. The microhardness of γ-Ni substrate was 450 MPa and that of Ni_3B was 650 MPa. The shear strength of the joint increased to 158 MPa as the brazing temperature increased to 1 120 ℃. The fracture surface displayed brittle features with some shearing dimples. Ni_3B interface formed between the super-Ni and brazed region. The joint fractured through the Ni_3B interface.

Key words: laminated composite; high-temperature brazing; microstructure; shear strength

Interface microstructure and mechanism of SiC ceramic vacuum brazed joint FENG Guangjie[1], LI Zhuoran[1], Xu Kai[1], LIU Wenbo[2] (1. State Key Laboratory of Advanced Welding and Joining, Harbin Institute of Technology, Harbin 150001, China; 2. AVIC Harbin Dongan Engine Co., Ltd, Harbin 150066, China). pp 13 - 16

Abstract: Vacuum brazing of SiC ceramic was conducted using Ti-Zr-Ni-Cu solder. The interface microstructure and its formation mechanism was investigated. Scanning electron microscope (SEM) was used to observe the joint microstructure and conduct local energy spectrum analysis. The results show that the products in the joint interface were mainly TiC, Ti_5Si_3, Zr_2Si, Zr(s,s), Ti(s,s) + Ti_2(Cu, Ni) and (Ti,Zr)(Ni,Cu) phases. The microstructure of the joint interface could be expressed as SiC/TiC/Ti_5Si_3 + Zr2Si/Zr(s, s)/Ti(s, s) + Ti_2(Cu,Ni)/(Ti,Zr)(Ni,Cu). The brazing process could be divided into five stages: physical contact between the solder and substrate, melting of solder and formation of reaction layer on the ceramic side, continuous diffusion of melted solder into the substrate, thickness increasing of reaction layer, composition homogenization, ending of reaction on ceramic side and formation of hypereutectic structure, solidification of intermetallic compounds in the center of joint. The shear strength of the joint brazed at 960 ℃ for 10min reached 110 MPa.

Key words: ceramic; vacuum brazing; microstructure; mechanism

Analysis of improving stability of welding technology by applying auxiliary electric field between slag and metal LI Xiaoquan, YANG Zonghui, ZHAO Zhiguo (School of Material Engineering, Nanjing Institute of Technology, Nanjing 211167,

China). pp 17 – 20

Abstract: To improve the stability of welding technology and reduce the post-weld repair due to defects like surface imperfections in key steel structure, a new method by applying auxiliary electric field between the slag and metal during submerged arc welding to guide electric current was developed. The electric signal instrument was used to collect arc voltages for statistics and analysis. The results show that the electric conductivity of molten slag can be improved with tungsten electrode as the cathode, and the electrons are guided into the arc centre to contract the welding arc. Meanwhile, positive and negative ions in the molten slag and weld pool metal migrated to the interface and combined into active oxides with low surface energy. Thus the wetting and spreading performance of molten slag on the surface of weld pool metal are improved. With the beneficial effect brought by the auxiliary electric field, the weld surface is smooth, the appearance of weld and especially the consistency of weld width are improved. Also, the welding process is more stable.

Key words: auxiliary electric field; submerged arc welding; welding processing; arc stability

Ultrasonic phased array inspection technology for defects in friction stir welded seam YU Liang, CHEN Yuhua, HUANG Chunping, GE Junwei, KE Liming (School of Aeronautical Manufacturing Engineering, Nanchang Hangkong University, Nanchang 330063, China). pp 21 – 24

Abstract: Ultrasonic phased array inspection technology was used to detect the defects in friction stir welded seam with different thicknesss. The inner defects were precisely quantified and represented by changing the scanning angle, focus depth and focus size of phased array. The morphology of the defects was observed by dissecting the welded seam with defect signal. The results show that the inner defects can be quickly determined with higher detection sensitivity probe. The position, size and distribution of the defects can be precisely detected through three views obtained by different scanning modes. The shape and peak value of echo signal were determined by the defect shape. The echo signal of little hole defect was a sharp peak and the peak value was large. The echo signals of aluminium coating and loose defects were multiple-cluster wave. In S-scan, the lightspots of loose defect were more intensive and distributed more widely than aluminium coating defect.

Key words: aluminium alloy; friction stir welding; ultrasonic phased array; weld defect

Joint characteristics of magnesium/steel dissimilar metals during bypass-current MIG welding-brazing MIAO Yugang, WU Bintao, HAN Duanfeng, XU Xiangfang, LI Xiaoxu (College of Shipbuilding Engineering, Harbin Engineering University, Harbin 150001, China). pp 25 – 28

Abstract: Bypass-current MIG welding-brazing of AZ31 magnesium alloy and Q235 galvanized steel was carried out. The results show that the technology could obtain stable welding process and good bead appearance. The optical microscopy, high-speed cameras and tensile testing machine were applied to observe and analyze the joint morphology, droplet transfer process and mechanical properties. It was found that the repelled transfer of droplet in the welding process prolonged the droplet transfer time, resulting in more uniformly wetting and spreading of droplet and integration of alloying elements in the interface. The tensile strength reached 133 MPa, about 70% of the base material. The joint fracture occurred in the magnesium weld, displaying ductile fracture features.

Key words: magnesium alloy; galvanized steel; bypass-current MIG welding-brazing; droplet transfer; welding characteristic

Effect of aging treatment on interfacial microstructure and mechanical properties of Sn-Zn-Ga-Nd soldered joints XUE Peng, XUE Songbai, SHEN Yifu (College of Materials Science and Technology, Nanjing University of Aeronautics and Astronautics, Nanjing 210016, China). pp 29 – 32

Abstract: The effect of aging treatment at 150 ℃ for different time on the interfacial microstructure and mechanical properties of Sn-Zn-Ga-Nd soldered joints was investigated. The results show that Ga could suppress the formation of Sn-Nd compound during the aging process and improve the reliability of soldered joints. The mechanical properties of the soldered joints further increased with the addition of Ga and Nd. The shear strength of soldered joints with Sn-Zn-Ga-0.08Nd decreased with increasing aging time, but was still remarkably higher than that of as-soldered joint with Sn-Zn solder.

Key words: aging treatment; soldered joint; interface; shear strength

Quality assessment using dynamic voltage characteristics in small scale resistance spot welding of titanium alloy ZHAO Dawei[1], WANG Xinyang[2], WANG Yuanxun[1], YANG Hao[1], ZHANG Lei[1] (1. Hubei Key Lab for Engineering Structural Analysis and Safety Assessment, Huazhong University of Science and Technology, Wuhan 430074, China; 2. Nanjing Kisen International Engineering Co., Ltd, Nanjing 210036, China). pp 33 – 36

Abstract: The voltage between the electrodes in small-scale resistance spot welding (SSRSW) of titanium alloy was collected by data acquisition system. The experiments revealed that the dynamic voltage signal included a lot of welding quality information. In order to demonstrate this finding and monitor the welding quality, the back-propagation artificial neural network (ANN) was employed to forecast the nugget diameter. The maximum predicted error of ANN was about 6.5%. Adjusting and monitoring the voltage waveform could be used to forecast the formation of weld nugget and monitor the quality of welded joints.

Key words: small-scale resistance spot welding; voltage waveform; quality monitoring; artificial neural network

Microstructure and mechanical properties of 5083 aluminum alloy joint by TIG welding CHEN Cheng[1], XUE Songbai[1], SUN Huhao[1], LIN Zhongqiang[2], LI Yang[1] (1. College of Materials Science and Technology, Nanjing University of Aeronautics and Astronautics, Nanjing 210016, China; 2. Zhejiang Yuguang Aluminum Material Co., Ltd, Wuyi 321200, China).